19th Australasian Fluid Mechanics Conference
Melbourne, Australia
8-11 December 2014

Direct Numerical Simulation of a Turbulent Lifted Flame: Stabilisation Mechanism

S. Karami[1] E. R. Hawkes[1,2], M. Talei[3] and H. Yu[4]

[1]School of Photovoltaic and Renewable Energy
The University of New South Wales, Sydney, NSW 2052, Australia

[2]School of Mechanical and Manufacturing Engineering
The University of New South Wales, Sydney, NSW 2052, Australia

[3]Department of Mechanical Engineering
University of Melbourne, Melbourne, VIC 3010, Australia

[4]Computer Science and Engineering
University of Nebraska-Lincoln, Lincoln, NE 68588, United States of America

Abstract

A turbulent lifted slot-jet flame is studied using direct numerical simulation (DNS). A single step chemistry model is employed with a mixture-fraction dependent activation energy to quantitatively reproduce the dependence of laminar burning rate on equivalence ratio that is typical of hydrocarbon fuels. It is observed that the leading flame edge exhibits a single branch close to the stoichiometric mixture fraction iso-surface, rather than a tribrachial structure. The flame edge has a complex, highly convoluted structure suggesting it can burn at speeds that are much faster than S_L. There is no evidence of a rich inner premixed flame or detached diffusion flame islands, in contrast with the observation in the previous DNS studies of hydrogen flames. On average, the streamwise velocity balances the streamwise flame propagation, confirming that flame propagation is the basic stabilisation mechanism. The analysis of the flow and propagation velocities reveal an elliptical pattern of flame motion around the average stabilisation point. Visualisation of the flame suggests that this motion is connected with the passage of large eddies.

Introduction

Flame stability is of critical importance in direct injection engines, gas turbines and many different types of combustion devices. As a result of a high jet velocity in these devices, the flame is abruptly lifted and stabilised at a downstream distance. The flame base in the lifted flame is a wrinkled ring fluctuating about a mean lifted height. Depending on the degree of turbulence and flow velocities at the jet inlet, rapid extinction and reignition might occur in the absence of an external ignition source or a bluff body. This local extinction may induce a flame blow off which is not desirable in combustion device. Therefore, lifted diffusion flames have been a topic of research for a long period of time. Nevertheless, the stabilisation mechanism in lifted flames is not fully understood. In the last five decades, different theories were proposed to explain the lifted-flame stabilisation mechanism. These theories may be classified as premixed flame, turbulent intensity, critical scalar dissipation, edge flame and large eddy theories [19, 15, 24, 23]. Recently, Gordon *et al.* [8] and Boxx *et al.* [3] observed the presence of flame islands upstream of the flame base in their experimental studies. They proposed that this structure is the consequence of the out-of-plane motion and it is the main reason for the flame-base jumps. The edge flame and large eddy theories received more attention in the literature. Therefore a brief discussion of these theories are presented here.

The edge-flame stabilisation mechanism was initially proposed by Buckmaster [5]. The edge flame is a premixed flame propagating in a quasi-laminar manner with the speed which has the same order of magnitude as the laminar flame speed. The edge-flame structures have been observed in several experimental studies [22, 25, 1, 2].

The stabilisation mechanism based on large eddy structures was first proposed by Broadwell *et al.*[4]. In this theory, the large structures cause re-entrainment of the hot products into the upstream fresh mixture and therefore stabilise the flame. In a separate scenario proposed by Miake-Lye *et al.* [16], the flame base propagates on the large scale structures in the turbulent lifted flames. This type of flame propagation has been reported in several other experimental studies of the non-premixed lifted flames [6, 23]. Lawn [14] proposed a different theory based on large structures. In this scenario, a large eddy departing from the fuel jet is diluted as moves toward the oxidiser stream. This flammable mixture reaches to the hot region and ignites. The ignited mixture then propagates in a form of an edge-flame or a triple flame upstream within the eddy while leaving the hot products behind for the next eddy to come.

The main conclusion from the literature is that there is no single theory being widely accepted to be accurate enough for prediction of the lifted height and also describing the stabilisation mechanism. Direct numerical simulation (DNS) provides a lot of information which is not easily accessible in the experiment. Therefore, this paper seeks to address the stabilisation mechanism of a turbulent lifted flame using the statistics of the flow and flame propagation at the flame base.

Numerical Method and Simulation Parameters

The conservation equations of mass, momentum, sensible energy and species are solved in non-dimensional form. These equations are nondimensionalised with respect to the inlet jet width, H, the speed of sound, temperature and thermodynamic properties on the jet centreline at the inlet. A single-step irreversible reaction of $F + rO \rightarrow (1+r)P$ where r is the stoichiometric ratio, *i.e.* the mass of oxidant disappearing with unit mass of fuel was used. The DNS code S3D_SC is employed here which is a modified version of the detailed chemistry code S3D [7]. The solver uses high-order accurate, low dissipative numerical schemes and a 3D structured, Cartesian mesh. The spatial derivatives were discretised using an 8^{th} order central differencing scheme and the time integration was performed with a 6-stage, 4^{th} order, explicit Runge-Kutta method. To suppress the numerical fluctuations at high wave numbers, a 10^{th} order filter [13] was applied every 10 time steps.

Non-reflecting outflow boundary conditions were used in the streamwise and transverse directions, and periodic boundary

Jet width	H
Domain size ($L_x \times L_y \times L_z$)	$16H \times 24H \times 8H$
Number of grid points ($N_x \times N_y \times N_z$)	$800 \times 800 \times 400$
Mean inlet jet Mach number (U_{jet})	0.48
Laminar co-flow Mach number ($U_{co-flow}$)	0.001
Jet non-dimensional temperature	2.5
Co-flow non-dimensional temperature	2.5
Jet Reynolds number	5,280
Inlet velocity fluctuation	5%
Fuel mixture fraction in fuel stream ($Y_{F,o}$)	1.0
Oxidiser mixture fraction in oxidiser stream($Y_{O,o}$)	0.233
Stoichiometric mixture fraction (Y_{Fst})	0.055
Stoichiometric oxidiser to fuel mass ratio r	4.0
Heat release parameter (α)	0.86
Ratio of specific heat (γ)	1.4
Baseline Zel'dovich number (β_0)	5.0
Non-dimensionisation Damköhler number (Da)	800.0
Prandtl number (Pr)	0.7
Lewis number ($Le = Sc/Pr$)	1.0

Table 1. Numerical and physical parameters of the simulation

conditions were applied in the spanwise direction. The simulation parameters along with their values are presented in table 1. The configuration is a slot jet flame similar to that studied in [27, 26]. The mean inlet axial velocity, $\mathrm{U_{in}}$ (and fuel mass fraction $\mathrm{Y_F}$), were specified using a tanh-based profile with an inlet momentum (and mixing layer) thickness, δ, is equal to 0.05H. To describe the velocity fluctuations at the inlet,u, a homogeneous isotropic turbulence field based on a prescribed turbulent energy spectrum with a turbulence intensity of 5% is first produced. These velocity fluctuations are then added to the mean inlet velocity using the Taylor's frozen turbulence hypothesis [27, 26].

A uniform grid spacing of $0.02H$ was chosen for the streamwise and spanwise directions. An algebraically stretched mesh was applied [9] in the transverse direction which maintained uniform spacing of $0.02H$ in $|y| < 7.5H$ and less than 3% of grid stretching in the region of $|y| > 7.5H$. The simulation was run for 18.0 jet flow through times, $t_j = L_x/U_j$ (where L_x is the length of the computational domain in the streamwise direction), and the data of the last $12.0t_j$ were used for analysis.

The turbulence resolution was assessed considering the Kolmogorov scale defined as $\tilde{\eta}_k = (\tilde{\nu}^3/\tilde{\varepsilon})^{1/4}$. The minimum $\tilde{\eta}_k/dx$ at the flame base is roughly 0.5 which is considered sufficient for DNS [21]. To evaluate the flame resolution, a laminar triple flame was simulated using the same parameters as the turbulent case. The thermal thickness was defined as, $\delta_{th} = (T_{ad} - T_o)/(\frac{\partial T}{\partial \xi})$, where T_{ad} is the adiabatic flame temperature, T_o is the unburned mixture temperature and ξ is the iso-line of mixture fraction corresponding to the maximum laminar flame speed. The thermal thickness was equal to 0.16 H, and there are 8 grid points across the flame, which is normally considered sufficient for a one-step chemistry DNS [11].

Results and Discussion

Flame Edge General Structure

The volume rendering of logarithm of the scalar dissipation rate (blue/white) and reaction rate (red/orange) is presented in figure 1. It may be observed that the flame has a complex structure which has features that are qualitatively similar to experimental observations of lifted flames [12, 3, 25]. Because the stoichiometric mixture fraction is small (0.055), the flame is found at the edge of the highly turbulent inner core of the jet. Heat release

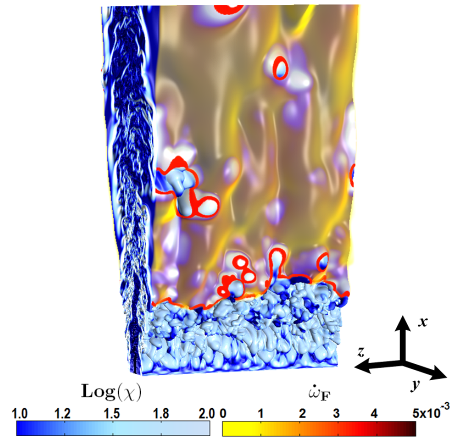

Figure 1. Three-dimensional volume rendering of logarithm of the scalar dissipation rate (blue/white) and reaction rate (red/orange). (Only the region $x/H < 14$ is shown.)

noticeably damps turbulence in the outer region. Unlike the hydrogen DNS of Mizobuchi *et al.* [18, 17], we do not observe a vigorous rich premixed flame core. We believe this difference is because hydrogen burns much more vigorously than hydrocarbons in rich mixtures. The mixture-fraction dependence is built into the present model by the mixture-fraction dependent activation energy. Similarly, we also did not observe any diffusion flame islands on the lean side that were observed by Mizobuchi *et al.* [18, 17]. Rather, we observe mostly a diffusion flame without a significant lean premixed branch. Once again this might have been a hydrogen-specific feature due to the very lean equivalence ratios that hydrogen can support a premixed flame.

The leading flame edges at the base of the flame are highly convoluted. Consistent with many experimental observations of lifted flames [12, 3, 25], the leading edges do not show a tribrachial structure. This lack of three distinct branches has been previously explained to result from mixture-fraction gradients ahead of the flame being too large to support distinct lean and rich branches [22]. The reaction rate is locally higher at the flame edges than further downstream, which is consistent with the existence of a premixed leading edge flame. It is also noted that in the present case, the premixed flame edges are quite narrow and of the order of the laminar flame thickness, which implies that the premixed edge flames are quite unlike a flat turbulent premixed flame.

There is a proliferation of flame holes, not observed in earlier DNS studies of lifted flames [18, 17, 27, 26]. Although the analysis of the holes is not the focus of this paper, it is noted here that the holes originate by two different mechanisms. Some of the holes are generated by flame propagation at the leading edge to surround an unburned region with burning regions while others are caused by local flame extinction. Both kinds of holes can either grow or shrink and disappear as they go downstream. They can also merge with other holes and split into multiple holes. The existence of extinction holes suggests that in this flame, the critical scalar dissipation rate can be locally exceeded, which suggests that extinction can moderate the stabilisation process [15].

We do not however observe any unconnected regions of high reaction rate ahead of the leading edge. All regions ahead of the leading edge are connected, even though in a two-dimensional (2D) streamwise-transverse plane they may appear as unconnected flame elements. Nor do we observe any transport of hot products or even large scale folding of the flame into upstream unburned regions. The lack of any unconnected regions

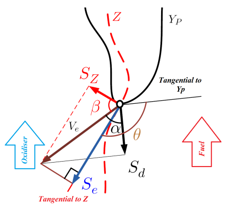

Figure 2. Schematic of edge flame propagation along the mixture fraction iso-surface.

or large scale folding of the flame to upstream regions therefore rules out, for the present flame, the large eddy theory of flame stabilisation, where it was proposed by Broadwell *et al.* [4] that wherein upstream turbulent transport of pockets of hot products caused the flame to stabilise. However, the stabilisation mechanism is also not entirely laminar. The large degree of convolution of the flame edge implies it can consume stoichiometric reactants at a much greater rate than in a laminar flame (which would present a single straight line here), similar to how increased surface area causes the turbulent burning velocity to be larger than the laminar one in premixed flames. Later in the article we will present evidence that large eddies definitely do play a role here.

Analysis of Edge Flame Velocities

The most advanced experiments that have investigated lifted flame stabilisation [3] have measured three components of the flow velocity in a time-resolved manner simultaneously with a flame marker such as planar laser-induced fluorescence (PLIF) of OH. These have provided very useful information; however, to the best of our knowledge, flame propagation speeds relative to the flow have never been measured. While the available data has suggested that flame propagation plays a key role, without access to both the flow and relative propagation speed, it has previously been impossible to demonstrate definitely that there is a balance between flame propagation and flow speeds.

To this end, the edge flame velocities have been extracted. The flame edge is defined as the intersection of a mixture-fraction iso-surface with a product mass-fraction iso-surface. The mixture-fraction iso-value was 0.07, which corresponds to the mixture-fraction having the highest laminar flame speed in a one-dimensional flat premixed laminar flame, while the product iso-value was selected as the value corresponding to the maximum reaction rate in this same flame. By analysing a large number of flame images, it was found that this always corresponded very well with the upstream leading edge of the flame as judged from the reaction rate, as well as with the edge flames around flame holes. With this definition, it is possible to analytically define the edge velocity. The net edge-flame velocity is given by:

$$\mathcal{U} = \boldsymbol{U} + \boldsymbol{V_e}, \tag{1}$$

where $\mathcal{U}$ is the net velocity in the laboratory frame, $\boldsymbol{U}$ is the flow velocity, and $\boldsymbol{V_e}$ is the displacement velocity of the flame relative to the flow. Previous work by the last author [10] demonstrated that $\boldsymbol{V_e}$ is given by:

$$\boldsymbol{V_e} = S_e\boldsymbol{T_2} + S_z\boldsymbol{N_z}. \tag{2}$$

This equation is best understood by consulting the diagram in figure2. The quantity S_e is the edge-flame displacement speed in the plane of the mixture-fraction iso-surface in the direction T_2, which is the tangent vector to the mixture-fraction iso-surface that is normal to the intersection line which defines the edge, pointing towards the unburned reactants. Here, S_e is given in terms of the product mass fraction self-displacement speed S_d, the mixture-fraction self-displacement speed S_z, and the inner product of the normal vectors to product and mixture-fraction

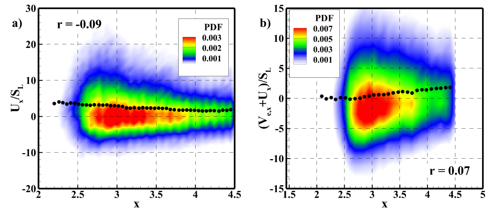

Figure 3. The joint PDF contours of a) streamwise flow velocity b)streamwise net velocity.

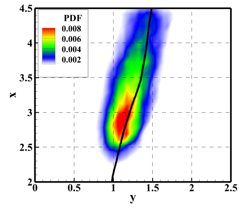

Figure 4. The PDF of the flame location points in a streamwise-transverse plane.

iso-surfaces k as:

$$S_e = \frac{S_d - kS_z}{\sqrt{(1-k^2)}}. \tag{3}$$

The iso-surface self-displacement speeds are given by [20]:

$$\rho_u S_z^* = \rho S_z = \frac{1}{|\nabla Z|}\left(-\frac{\partial}{\partial x_j}\left(\frac{\mu}{ReSc}\frac{\partial Z}{\partial x_j}\right)\right), \text{ and} \tag{4}$$

$$\rho_u S_d^* = \rho S_d = \frac{1}{|\nabla Y_P|}\left(-\dot{\omega}_P - \frac{\partial}{\partial x_j}\left(\frac{\mu}{ReSc}\frac{\partial Y_P}{\partial x_j}\right)\right),$$

It is then apparent that $S_z\boldsymbol{N_z}$ is the flame displacement in the mixture fraction direction. Results are now presented for these various speeds. First, figure3a shows the probability density function (PDF) and mean streamwise velocity U_x, conditioned on the streamwise location. The key points to note are that the mean velocity is positive and the order of a few S_L, and that fluctuations of velocity are significant relative to the mean. Next, figure3b shows the PDF and mean streamwise net velocity $\mathcal{U}_x$ conditioned on streamwise direction. The fact that the conditional mean of this quantity is nearly zero shows that the flow in net balances the flame propagation, thus demonstrating that flame propagation is the mechanism that controls the flame stabilisation. However, even after adding in the relative flame displacement speed, fluctuations are still significant. The sources of the fluctuations are therefore now examined in more detail. Figure 4 shows the PDF of the flame location points in a streamwise-transverse plane, and the stoichiometric mean mixture fraction contour. It shows that the flame is stabilised around x=3.2H and y=1.2H, near the mean stoichiometric location, and experiences fluctuations that are larger in the direction aligned tangential to the mean stoichiometric contour than the direction normal to it. To explain these fluctuations of the lifted height location, figure5a shows the net streamwise edge-flame velocity conditioned on the flame location while figure5b shows the transverse component. These figures clearly show that the flame tends to move on average in an elliptical pattern around the mean stabilisation location. On the on-average lean side, the streamwise velocity component is negative, moving the flame downstream. Once it reaches the downstream location, it then moves inwards, where it encounters a region of high positive streamwise velocity which pushes it downstream again. Finally, it encounters a positive transverse velocity, moving it outwards to the on-average lean side again. (It is important to understand that the phrase on-average lean side is used rather than simply lean side, because instantaneously the flame is always found on the stoichiometric surface.) It is proposed that this pattern is connected with the passage of large eddies. Starting at the 3 o'clock location on the lean side, the flame is proposed to exist on the outer side of a clockwise-rotating large eddy. The large

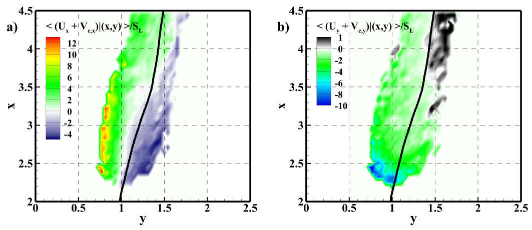

Figure 5. a) the net streamwise edge-flame velocity conditioned on the flame location and b) the net transverse edge-flame velocity conditioned on the flame location.

eddy plus the flame propagation move the flame downstream while the centre of the eddy which is some distance away towards the centre of the jet is moving downstream. As the large eddy passes the flame, the trailing edge of the eddy rapidly entrains the flame into the centre of the jet through 6 o'clock where it encounters a region of high streamwise velocity which pushes the flame downstream again at 9 o'clock. Eventually it encounters another large eddy which moves it outwards again through 12 o'clock and then the eddy moves it down to 6 o'clock again. Overall, this picture is very consistent with several other proposals in the literature, notably those of Miake-Lye *et al.* [16] and Su *et al.* [23]. The role of large eddies is also consistent with observations of lifted flames in autoignitive conditions, where they moderate the autoignition stabilisation mechanism [27, 26].

Conclusions

A direct numerical simulation modelling a lifted, slot-jet flame in a cold oxidiser environment has been presented. In order to achieve a relevant parameter space in terms of Reynolds and Damkhler numbers, a simple one-step chemistry model was used with an adjusted activation energy to qualitatively reproduce the strong equivalence ratio dependence of burning velocity that is typical of hydrocarbon flames. The following conclusions are drawn about the stabilisation of the flame:

- Features of a rich inner premixed flame and diffusion flame islands previously from a hydrogen DNS are not observed, suggesting these features were specific to hydrogen which can support a premixed flame at much lower and higher equivalence ratios than hydrocarbons.

- The stabilisation region is instead shown to involve partially-premixed, single-branched edge flames. The flame edge has a complex, highly convoluted structure suggesting it can burn at speeds that are in net faster than S_L.

- The streamwise flow is shown to balance the streamwise flame propagation on average, therefore the flame propagation is the basic stabilisation mechanism.

- There are significant fluctuations in lifted height and conditioning of the net flame velocity on streamwise and transverse location reveals an elliptical pattern of flame motion around the average stabilisation point. The motion is clockwise on the right-hand side of a vertical flame. It is proposed that the clockwise on-average motion is connected with the passage of large eddies.

- There also is evidence of local extinction holes as well as flame holes suggesting that a critical scalar dissipation corresponding the appearance of negative displacement speed moderates the process. (An analysis, not shown in this appear, however suggests it is a moderating factor rather than a fundamentally controlling one.)

Future work will consider whether these conclusions are dependent on parameters including the lifted height, dilution, Lewis number, and configuration (round/slot jet).

Acknowledgements

The research benefited from computational resources provided through the National Computational Merit Allocation Scheme, supported by the Australian Government. The computational facilities supporting this project included the Australian NCI National Facility, the partner share of the NCI facility provided by Intersect Australia Pty Ltd., and the UNSW Faculty of Engineering.

References

[1] Arndt, C. M., Schiel, R., Gounder, J. D., Meier, W. and Aigner, M., *Proc. Combust. Inst.*, **34**, 2013, 1483 – 1490.

[2] Boulanger, J., Vervisch, L., Reveillon, J. and Ghosal, S., *Combust. Flame*, **134**, 2003, 355–368.

[3] Boxx, I., Heeger, C., Gordon, R., Böhm, B., Aigner, M., Dreizler, A. and Meier, W., *Proc. Combust. Inst.*, **32**, 2009, 905–912.

[4] Broadwell, J. E., Dahm, W. J. and Mungal, M. G., *Symposium (International) on Combustion*, **20**, 1985, 303–310.

[5] Buckmaster, J. and Weber, R., *Symposium (International) on Combustion*, **26**, 1996, 1143 – 1149.

[6] Burgess, C. P. and Lawn, C. J., *Combust. Flame*, **119**, 1999, 95–108.

[7] Chen, J., Choudhary, A., De Supinski, B., Devries, M., Hawkes, E., Klasky, S., Liao, W., Ma, K., Mellor-Crummey, J., Podhorszki, N., Sankaran, R., Shende, S. and Yoo, C., *Comput. Sci. Disc.*, **2**.

[8] Gordon, R. L., Boxx, I., Carter, C., Dreizler, A. and Meier, W., *Flow Turbul. Combust.*, **88**, 2012, 503–527.

[9] Hawkes, E. R., Chatakonda, O., Kolla, H., Kerstein, A. R. and Chen, J. H., *Combust. Flame*, **159**, 2012, 2690 – 2703.

[10] Hawkes, E. R., Sankaran, R. and Chen, J. H., *Proc. Combust. Inst.*, **33**, 2011, 1447–1454.

[11] Hesse, H., Chakraborty, N. and Mastorakos, E., *Proc. Combust. Inst.*, **32**, 2009, 1399–1407.

[12] Joedicke, A., Peters, N. and Mansour, M., *Proc. Combust. Inst.*, **30**, 2005, 901–909.

[13] Kennedy, C. A. and Carpenter, M. H., *Appl. Numer. Math.*, **14**, 1994, 397 – 433.

[14] Lawn, C. J., *Prog. Energy Combust. Sci.*, **35**, 2009, 1–30.

[15] Lyons, K. M., Watson, K. A., Carter, C. D. and Donbar, J. M., *Combust. Sci. Technol.*, **179**, 2007, 1029–1037.

[16] Miake-Lye, R. C. and Hammer, J. A., *Proc. Combust. Inst.*, **22**, 1989, 817–824.

[17] Mizobuchi, Y., Shinio, J., Ogawa, S. and Takeno, T., *Proc. Combust. Inst.*, **30**, 2005, 611–619.

[18] Mizobuchi, Y., Tachibana, S., Shinio, J., Ogawa, S. and Takeno, T., *Proc. Combust. Inst.*, **29**, 2002, 2009–2015.

[19] Pitts, W. M., *Combust. Flame*, **76**, 1989, 197–212.

[20] Pope, S., *Int. J. Eng. Sci.*, **26**, 1988, 445–469.

[21] Pope, S. B., *Turbulent Flows*, Cambridge University Press, 2000.

[22] Strner, S. H., Bilger, R. W., Frank, J. H., Marran, D. F. and Long, M. B., *Combust. Flame*, **107**, 1996, 307 – 313.

[23] Su, L. K., Sun, O. S. and Mungal, M. G., *Combust. Flame*, **144**, 2006, 494–512.

[24] Upatnieks, A., Driscoll, J. F., Rasmussen, C. C. and Ceccio, S. L., *Combust. Flame*, **138**, 2004, 259 – 272.

[25] Watson, K. A., Lyons, K. M., Donbar, J. M. and Carter, C. D., *Combust. Sci. Technol.*, **175**, 2003, 649–664.

[26] Yoo, C. S., Richardson, E. S., Sankaran, R. and Chen, J. H., *Proc. Combust. Inst.*, **33**, 2011, 1619–1627.

[27] Yoo, C. S., Sankaran, R. and Chen, J. H., *J. Fluid Mech.*, **640**, 2009, 453–481.